Algal Research 40 (2019) 101490

Contents lists available at ScienceDirect

Algal Research

journal homepage: www.elsevier.com/locate/algal

Pseudomonas sp. strain WJ04 enhances current generation of *Synechocystis* sp. PCC6803 in photomicrobial fuel cells

Wenjing Wang, Yanqing Sheng*

Key Laboratory of Coastal Zone Environmental Processes, Yantai Institute of Coastal Zone Research, Chinese Academy of Sciences, Yantai 264003, PR China
Center for Ocean Mega-Science, Chinese Academy of Sciences, 7 Nanhai Road, Qingdao 266071, PR China

ARTICLE INFO

Keywords:
Bacteria
High-throughput sequencing
Metabolomics
Photomicrobial fuel cells
Synechocystis

ABSTRACT

Photomicrobial fuel cells (pMFCs) are a new technology for transforming the light energy or bioenergy of algae into bioelectricity. However, the current methods of generating algal pMFCs have poor efficiency due to the complex electron transfer network in algal cells. In this study, pMFCs containing the model electricity-producing cyanobacterium *Synechocystis* sp. PCC6803 contaminated by additional bacteria exhibited a 12.6-fold greater voltage output compared to the control pMFCs with axenic *Synechocystis* sp. PCC6803. To explain this phenomenon, the compositions of symbiotic bacterial communities in bacterial-contaminated pMFCs were analyzed, and a pure strain WJ04 belonging to the genus *Pseudomonas*, which was the second most abundant (30.2%) among the total symbiotic bacteria, was obtained. The strain WJ04 was able to raise the voltage output by 8.3 fold compared with the control treatments, meaning that strain WJ04 contributed to the increased voltage output of pMFCs. Through the coculture experiment, strain WJ04 was found to influence the growth of *Synechocystis*, improve photosynthesis rates by regulating algal genes and further affect algal metabolite production compared with control treatments. In addition, nicotinamide, L-homocysteic acid and 4-aminobutyric acid (*fold change analysis*, *F.C.* ≥ 10) could regulate algal gene expression and enhance the coculture current density by 6.1–12.3 fold compared with the control treatments. Thus, these results provide a clear explanation for the high current production in bacterial-contaminated pMFCs, clarify the interaction mechanisms between algae and bacteria in the anode and provide accurate evidence for the role of bacteria in improving algal bioelectricity utilization.

1. Introduction

The billions of algae and bacteria distributed in rivers, lakes and oceans perform important ecological functions [1]. Algae are primary producers that can consume organic matter and release O_2 and extracellular polysaccharides into aquatic systems, and bacteria decompose organic matter and provide inorganic matter for primary producers [2–4]. Algae and bacteria represent an inseparable system and are found together in loose or tight association. The interactions between algae and bacteria in the phycosphere never occur in isolation, and the balance between various mutually beneficial cooperative and inhibitory processes may affect the survival of specific algae or bacteria at particular times, such as during phytoplankton blooms [5,6]. Microbial fuel cells (MFCs) and photoMFCs (pMFCs) are good systems for studying the oxidation-reduction reactions of interspecies interactions. Bioelectricity can be captured from algal and bacterial fuel cells and is expected to replace fossil fuels [7,8]. MFCs and pMFCs have become a research focus and have been applied in the search for new sustainable energy sources [9–11].

Increasing numbers of electricigens have been found in recent years, including *Geobacter* spp., *Shewanella* spp., *Rhodoferax ferrireducens*, *Pseudomonas aeruginosa* and *Thermincola potens*, which are common electricigens that can release electrons into the environment during respiration. Compared with bacteria, electrogenic algae are applied using bioelectrochemical technology that generates electrical energy and expends less energy. Algae can gain energy from sunlight and fix carbon dioxide to perform photosynthesis, release oxygen into the environment, and provide lipids [12–14]. Algae require less energy intake than bacteria due to photosynthesis, although cyanobacteria have complex electron transfer networks that are mainly adapted for light harvesting and not for electron output. The photosynthetic reactions of cyanobacteria are stacked to maximize the light-harvesting capacity of

* Corresponding author at: Key Laboratory of Coastal Zone Environmental Processes, Yantai Institute of Coastal Zone Research, Chinese Academy of Sciences, Yantai 264003, PR China.
E-mail address: yqsheng@yic.ac.cn (Y. Sheng).

https://doi.org/10.1016/j.algal.2019.101490
Received 14 November 2018; Received in revised form 3 April 2019; Accepted 3 April 2019
Available online 09 April 2019

the cell [15], and they deplete electrons from the algal electron transfer network and reduce the extracellular electron transfer process. Many terminal electron sinks are used to protect cyanobacteria from high levels of light and reduce stress [16,17]. With respect to electrogenic activity, these pathways are considered wasteful alternatives for electrons. Therefore, it is important to research new technology to improve the electron output of algae and convert light energy into electrical energy with high efficiency.

In laboratory environments, axenic algae are easily contaminated by bacteria because these organisms have a close relationship via their complementary physiologies and metabolic activities [18–20]. Cyanobacteria are among the most extensively studied types of algae, and many symbiotic bacterial communities live with algal cells [21]. Beneficial and harmful interactions occur between cyanobacteria and heterotrophic bacteria, including the promotion or inhibition of algal growth, protection from harmful environments, and provision of vitamins to the algae [22–24]. Studies on algal-bacterial interactions always address algal growth promotion and ignore the influence of the interactions on energy flow. Microorganisms always depend on electron transfer to discharge or capture energy, to cause chemical changes inside the cell and to provide micronutrients, including electrons, for their accompanying bacteria or algae. Kimura and Okabe (2013) [25] found that electron transfer activity between *Geobacter sulfurreducens* and *Hydrogenophaga* sp. AR20 can be enhanced through the addition of quinone compounds. *G. sulfurreducens* and *Prosthecochloris aestuarii* can also transfer electrons during syntrophic anaerobic photosynthesis [26]. Here, symbiotic bacteria may catalyze algal metabolic processes, whether nutrient or energy changes, to release more electrons into the anode chamber.

Synechocystis sp. PCC6803, a cyanobacterium, has poor light-dependent electrogenic activity and produces voltages up to 0.84–3.5 μA in axenic culture [27,28]. However, voltage generation in the pMFCs of *Synechocystis* contaminated by bacteria was higher than that in axenic pMFCs. In this study, this phenomenon was clarified by illuminating the bacterial community composition using high-throughput sequencing, explaining the interactions between *Synechocystis* and bacteria via reverse transcription-quantitative polymerase chain reaction (RT-qPCR) and identifying the differential metabolites via a HILIC ultra-high-pressure liquid chromatography mass spectrometry analysis.

2. Material and methods

2.1. pMFC devices

Both the anodes and cathodes of pMFCs were constructed with 100 mL glass bottles, and a cation exchange membrane (ULTREX-CMI-7000, USA) was used to separate the two chambers (Fig. 1A). Carbon cloths (HCP 330, Hesen, China) with an effective surface area of 10 cm^2 were heated using a muffle furnace, soaked in acetone and placed into the chambers as electrodes. The electrodes were connected by a titanium wire with an external resistor of 1000 Ω. The cathode chamber was filled with 50 mM potassium ferricyanide solution in 100 mM phosphate-buffered saline buffer (pH 7.1). A digital multimeter (Model 2700, Keithley, Tektronix, USA) was used to record the output voltage. Cyclic voltammetry curves were determined with an electrochemical workstation (CHI660D, Shanghai, Chenhua, China). An Ag/AgCl reference electrode was used to record the individual electrode potentials. Six repetitions of all treatments were incubated at 25 ± 1 °C with a 12–12 h light-dark illumination cycle. The pMFCs were operated under open circuit conditions for 7 days until the open circuit voltage stabilized.

2.2. Algal and bacterial strains

Synechocystis sp. PCC6803 was obtained from the Freshwater Algae Culture Collection at the Institute of Hydrobiology (Wuhan, China) and purified to eliminate bacterial contamination [29]. Bacterial DNA was stained with 4′,6-diamidino-2-phenylindole, and bacterial cell counts were controlled to remain below 0.1% of the total (algae and bacteria) cell count. Axenic *Synechocystis* sp. PCC6803 was then cultured in pMFCs as the control treatment. The other strain *Synechocystis* sp. was collected from a 6-month-old continuous culture tank, which had stable symbiotic bacteria communities, and was cultured in pMFCs as the coculture treatments. The strains were grown using standardized BG-11 medium, and the pH was adjusted to 7.1 with 1 mol L^{-1} NaOH and HCl. Algae were cultured at 25 °C under an illumination intensity of 25 μE s^{-1} m^{-2} in a constant temperature incubator with a cold light illuminator (GXM-258A, Ningbo Jiangnan, China). The photoperiod was 12 h, and the initial concentration of algae was set to 6 × 10^5 cell mL^{-1}.

2.3. High-throughput sequencing of bacteria in cocultured pMFCs

Samples were taken from the coculture pMFCs at the beginning of the experiment (day 0) and at day 10 according the method of Shen et al. (2011) [30]. The method of Krohn-Molt et al. (2017) [31] was used to separate the heterotrophic bacteria from the *Synechocystis* in the samples. To obtain total RNA, the bacteria were mixed with ice-cold buffer (50 mM Tris-HCl, 20 mM $MgCl_2$, pH 7.0), homogenized at 5.5 m s^{-1} for 45 s, and then centrifuged at 13,000*g* at 4 °C, for 5 min. The supernatants were retained, and the precipitates were resuspended with a lysis buffer and homogenized for 10 s. After centrifuging again, the new supernatants were combined with the supernatant from the first centrifugation, and the mixed supernatants were extracted sequentially with phenol: chloroform: isopentane (25:24:1) and then chloroform: isopentane (24:1). The aqueous phase and organic phase were separated, and the organic phase was discarded. The aqueous phase was added to sodium acetate and ethanol at −80 °C and incubated for 1 h. The solutions were centrifuged, washed with ethanol and air dried. TE buffer was used to dissolve the extractions, which were then quantified by an ultralow volume spectrometer (BioDrop μLite, Cambridge, England), verified on a 1.0% formaldehyde-agarose gel and stored at −80 °C. cDNAs were generated with the remaining extractions using a reverse transcriptase kit according to the manufacturer's instructions (Roche, Germany). The double-stranded DNA was amplified by polymerase chain reaction (Eppendorf, Germany). The products from the polymerase chain reaction were sent to the Novogene Company (Beijing, China) and analyzed by high-throughput sequencing using a HiSeq PE250 system.

2.4. Characteristics of strain WJ04

Carbon cloths were collected from the coculture treatments at the end of experiment and washed with sterile water to obtain the electricigens, which were then cultured in sodium citrate medium (3.0 g L^{-1} sodium citrate, 0.53 g L^{-1} NaCl, 2.0 g L^{-1} KH_2PO_4, 0.76 g L^{-1} $MgSO_4$, 0.01 g L^{-1} $CaCl_2$, 0.03 g L^{-1} $FeCl_3$) by spreading the bacteria-containing solutions on solid sodium citrate medium. After 1–2 weeks of incubation, strain WJ04 was isolated, purified, and transferred into modified Giltay medium [32]. The 16S rDNA of strain WJ04 was amplified using the primers 27F (5′-AGAGTTTGGATCMTG GCTCAG-3′) and 1492R (5′-TACGGYTACCTTGTTACGACTT-3′). The PCR products were purified and sequenced by Invitrogen (Invitrogen, China).

The electrochemical properties of strain WJ04 were detected in the pMFCs. Bacterial cells in the pMFCs were collected, dried and mixed thoroughly with approximately 100 mg of desiccated KBr under infrared radiation. The mixtures were pressed into tablets, and their infrared spectra were recorded with a Perkin-Elmer Spectrum One B Fourier transform infrared system (Japan, Jasco, FT/IR-4100). The FT/IR spectra were obtained in the wavenumber range of 4000–400 cm^{-1} and analyzed according to the methods of Lentini et al. (2016) [33] and Lee et al. (2017) [34], and the spectra were baseline-corrected and

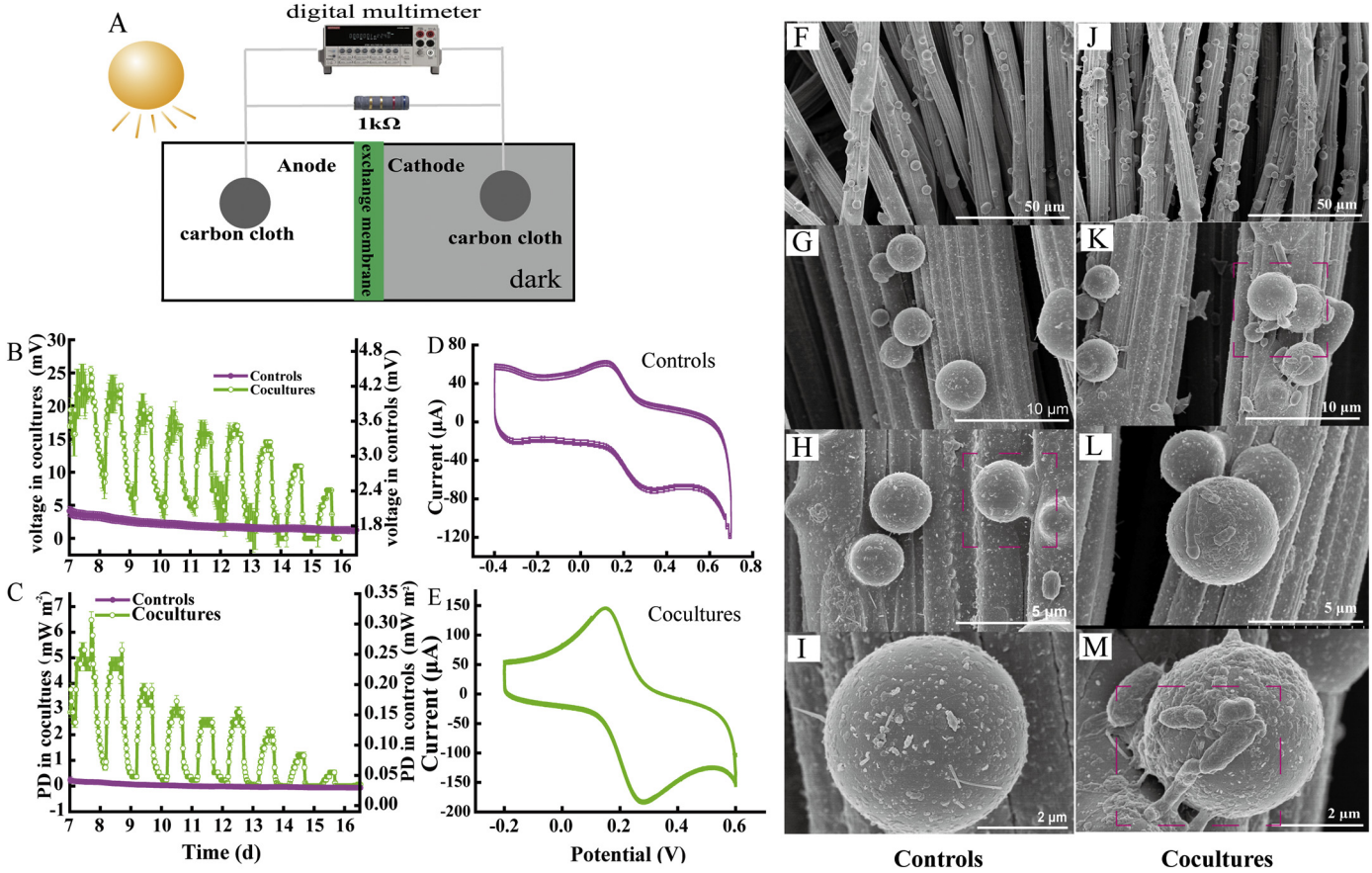

Fig. 1. Heterotrophic bacteria enhance the current production of algae pMFCs. (A) Two chambers pMFCs; (B–C) voltage and power density (PD) of the control (axenic *Synechocystis* sp. PCC6803) and coculture (bacterial-contaminated *Synechocystis* sp. PCC6803) treatments; (D–E) cyclic voltammetry curves of control and coculture treatments (three cycles); (F–I) SEM images of carbon cloth in control cultures; and (J–M) SEM images of carbon cloth in cocultures. Data are shown as the mean value (± S.E.), n = 3.

Table 1
Primers for RT-qPCR.

Primer	Forward (5′-3′)	Reverse (5′-3′)
16S rRNA	*AGAGTTTGATCCTGGCTCAG*	*AAGGAGGTGATCCAGCCGCA*
psbA	*GGTCAAGARGAAGAAACCTACAAT*	*GTTGAAACCGTTGAGGTTGAA*
ccmK	*TGACCGCTGGCATTGAAA*	*GGCGGATGATGGAAGGATTA*
speB	*ACCCAGGAAACGGACTTAG*	*GCCAACCACCAATGCCTAA*
ndhB	*ATGACGGACGCTCGACC*	*TCATATTAATACCGAGCT*
petJ1	*TCAAACCCACCAGGG*	*ATGGATAACACACAGGCG*
cytM	*GATGAGACGGATTTGGGAATGGC*	*GGAAGGTTCATTTTTGAG*
fdhF	*GATTAACTGGAGCGA GACC*	*TCCGAAAGGAGGCTG TAG*
nox5	*TCAGTACGCAGAGGTCCAGGT*	*GGCATCGACCATCTCCACTTC*
nox1	*CAATGGCACCCNTTTACCATA*	*GCNGGACTNCCATATGG*
psbB	*GTGCTATGAACAGTGGTGATGGC*	*TTTAGACTCGGAACGACGGAAGG*
hlyD	*ATCGGGTACCATGAATAGCCCCACC*	*ATCGAGACTCCTAACGAACAGTTTC*

normalized to 1.0 for comparison.

2.5. Cocultivations of Synechocystis and strain WJ04

Interactions between the algae *Synechocystis* and strain WJ04 were determined in coculture treatments as described by Song et al. (2017) [35]. Dialysis bags (pore size 8000–14000, 25 mm × 5 mm; Solarbo, Beijing, China) were used to insulate algae from bacteria in the co-culture treatments (Fig. S1). To ensure the consistency of the results, each treatment was performed with six replicates. Dialysis membrane tubes were cut into approximately 20 cm sections and then soaked and boiled in 2% (w/v) $NaHCO_3$ and 1 mmol L^{-1} EDTA (pH 8.0) solution for 10 min. Then, the tubes were washed with sterile distilled water and boiled again with 1 mmol L^{-1} EDTA (pH 8.0) for 15 min. After cooling, the tubes were stored at 4 °C. The dialysis membrane tubes were washed with sterile distilled water before the experiments. At the beginning of each experiment, the cocultures were inoculated with 6×10^5 cell mL^{-1} algae and 10 mL bacteria with 6×10^8 cell mL^{-1}. The bacteria were placed into dialysis membrane tubes. The experimental treatments with no bacteria added to the dialysis membrane were considered the control treatments. Algal cells were counted with a light microscope (Olympus BX51, Tokyo, Japan). The chlorophyll fluorescence parameters were measured with a multiple excitation wavelength-modulated chlorophyll fluorescence instrument (Multi-Color-PAM, USA).

2.6. RT-qPCR analysis

On day 10, *Synechocystis* cells were collected from the control and coculture treatments through centrifugation (5000*g*, 4 °C) and used to detect the gene expression related to the electron transfer networks (Table 1). 16S rRNA transcript levels were used as reference sequences. The liquid was removed from the surfaces of the *Synechocystis* cells as much as possible. For every 5×10^6 algal cells, 1 mL of TriQuick reagent (Solarbio, China) was added to the samples. Glass homogenizers were used to homogenize and fully disrupt the cells to obtain the total RNA. The RNA was further purified using RNA purification kits (QIAGEN, Hilden, Germany), and the integrity of the rRNA was evaluated using agarose gel electrophoresis. An ultralow volume spectrometer (BioDrop μLite, Cambridge, England) was used to determine the RNA concentration. cDNA was transcribed using reverse transcription kits (Invitrogen, USA). The 20 μL RT-qPCR reactions contained the following: 2 μL dNTPs, 0.3 μL Taq, 14.2 μL ultra-pure water, 2 μL 10× buffer (Mg^{2+}), 1.5 μL cDNA, 1 μL primers and sterile DEPC water. RT-qPCR was performed using a SYBR Green PCR kit (Toyobo, Japan) and a Chromo4 Real-Time Detection System (MJ Research, Cambridge, MA). The relative abundances in the different samples were determined and the *Synechocystis* 16S rRNA values in the control treatments were set to 1. Six replicates were performed for all treatments.

2.7. Metabolomic analyses

Equivalent samples were collected from the six replicates of control and coculture treatments. Algal cells were washed with PBS and centrifuged at 5000*g* at 4 °C for 5 min. The supernatants were discarded, and the precipitates were collected in 1.5 mL centrifuge tubes, quickly frozen in liquid nitrogen and stored at −80 °C until analysis. For analysis, the samples were slowly thawed at 4 °C and 1 mL of methanol-acetonitrile-water (2:2:1, v/v) was added with a sufficient vortex using an Agilent 1290 Infinity LC system with a Triple TOF 5600+ mass spectrometer (AB SCIEX). The chromatographic conditions were as follows: samples were separated on an ACQUITY UPLC BEH amide chromatographic column (1.7 μm, 2.1 mm × 100 mm) using an Agilent 1290 Infinity LC UHPLC; the column temperature was 25 °C; the flow rate was 0.3 mL min^{-1}; the input volume was 2 μL; mobile phase A was composed of 26 mM ammonium acetate and 26 mM ammonia in water; and mobile phase B was composed of acetonitrile. The gradient program was as follows: 5% A, 0–1 min; 5–35% A, 1–14 min; 35–60% A, 14–16 min; 60% A, 16–18 min; 60% A-5% A, 18–18.1 min; and 5% A, 18.1–23 min. The samples were stored at 4 °C. Components in the separated samples were detected with the ESI positive and negative ion modes of the Triple TOF 5600+ mass spectrometer. The ESI conditions were as follows: ion source gas 1(Gas1): 60; ion source gas 2 (Gas2): 60; curtain gas (CUR): 30; source temperature: 600 °C, ion spray voltage floating (ISVF) ± 5500 V (positive and negative ion modes); TOF MS scan *m/z* range: 60–1000 Da; product ion scan *m/z* range: 25–1000 Da, TOF MS scan accumulation time: 0.20 s/spectra; product ion scan accumulation time: 0.05 s/spectra; declustering potential (DP): ± 60; collision energy: 35 ± 15 eV (excluding isotopes within 4 Da); and candidate ions to monitor per cycle: 6. Additionally, secondary mass spectrometry was obtained by information dependent acquisition (IDA) using the high sensitivity mode.

2.8. Metabolites influence algal current generations

Nicotinamide, L-homocysteic acid and 4-aminobutyric acid were separately dissolved in sterile water at a concentration of 0.1 mg L^{-1}. The solutions were filtered using 0.22 μm membrane filters. Then, 1 mL of the nicotinamide, L-homocysteic acid and aminobutyric acid solutions were separately added to the algal cultures. The cultures that contained no metabolites or algae were considered as control treatments. A digital multimeter was used to record the output voltage every 5 min. After sampling, the algal cell counts were calculated in a counting chamber using a light microscope (Olympus BX51, Tokyo, Japan). The gene expressions of the algae in the different treatments were determined by RT-qPCR. The specific primers used are shown in Table 1.

2.9. Statistical analyses

Mothur and USEARCH were used to treat the raw sequence data from high-throughput sequencing; and other standard statistical analyses and graphics were performed using Microcal™ Origin 9.0 (Micro Cal Software Inc. USA). Phylogenetic trees were structured using MEGA 5.0. All 16S rRNA gene sequences obtained in the study have been deposited in the GenBank Data Library. Student's *t*-test was performed using SPSS Version 16.0.

Raw metabonomics data were converted to the mzXML format by ProteoWizard. Peak alignments, peak retention time adjustments and peak area calculations were accomplished by the program XCMS. The resulting data were analyzed using Simca-p 14.1 (Umetrics, Umea, Sweden) and Pareto scaling. The structures of the metabolites were identified by accurate mass number matching (< 25 ppm) and secondary spectrum matching, and the metabolites were searched in the self-built database in the laboratory. For the data extracted by XCMS, the ion peaks whose missing values were > 50% were deleted. SIMCA-P 14.1 (Umetrics, Umea, Sweden) was used to perform the mode identification, Pareto scaling and data preprocessing, and then multi-dimensional statistical analyses, including unsupervised principal component analysis (PCA), supervised partial least squares discriminant analysis (PLS-DA) and orthogonal partial least squares discriminant analysis (OPLS-DA), were carried out. One-dimensional statistical analyses, such as Student's *t*-test and variation fold change analysis, were also performed, and the software R was used to draw the volcanic map.

3. Results and discussion

3.1. Symbiotic bacteria improve algal current generation

In this study, voltages from the control and coculture treatments were recorded using a data acquisition unit with a consistent external resistance. Voltages were recorded under closed circuit conditions following preincubation for seven days until the open circuit voltage stabilized. The voltages in the coculture values were up to 12.6-fold higher than those in the control treatments (Fig. 1B & Fig. S2). The maximum voltage was 25.2 mV in the cocultures and 2.0 mV in the control cultures (Fig. 1B). Moreover, regular diurnal variation of the voltage output was observed in the control and coculture treatments, which is consistent with the complex electron transfer networks that are involved in algal photosynthesis and respiration. The highest voltage was approximately 2.1-fold greater than the lowest current density in the cocultures. This change in voltage related to illumination is common in algae but not in bacteria [36]. However, symbiotic photosynthetic bacteria in cocultures that could contribute electrons were not eliminated and should not be ignored. Power densities were also higher in cocultures than in control treatments (Fig. 1C). Cyclic voltammetry curves from an electrochemical workstation showed an obvious potential oxidation and reduction peak in the cocultures (Fig. 1D) but not in the control treatments (Fig. 1E). Carbon cloth electrodes were observed by scanning electron microscopy (SEM). The images revealed that *Synechocystis* cells in the control treatments were attached to the carbon fibers (Fig. 1F–I). When the carbon cloth was further magnified, a trochal disc form of *Synechocystis* cells were obviously adhered to the electrodes. Heterotrophic bacteria in the coculture treatments attached tightly to the carbon cloths and the surfaces of the algal cells (Fig. 1J–M). Algae, bacteria and electrodes can be tightly associated or used as a “wire” structure to link to each other, thereby shortening the

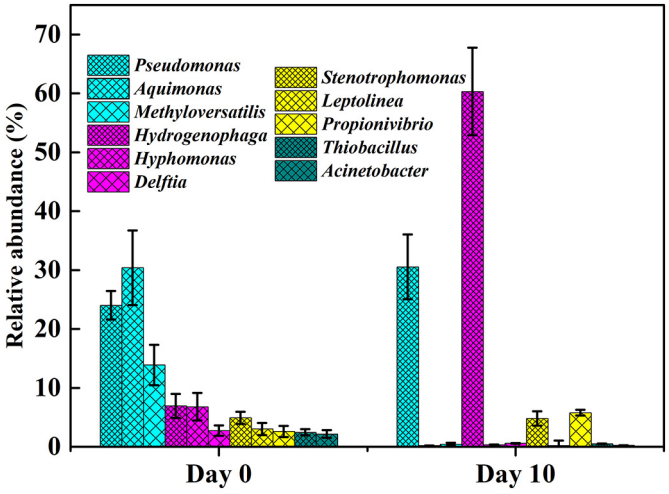

Fig. 2. Mean (± S.E., n = 3) relative abundances of bacterial communities.

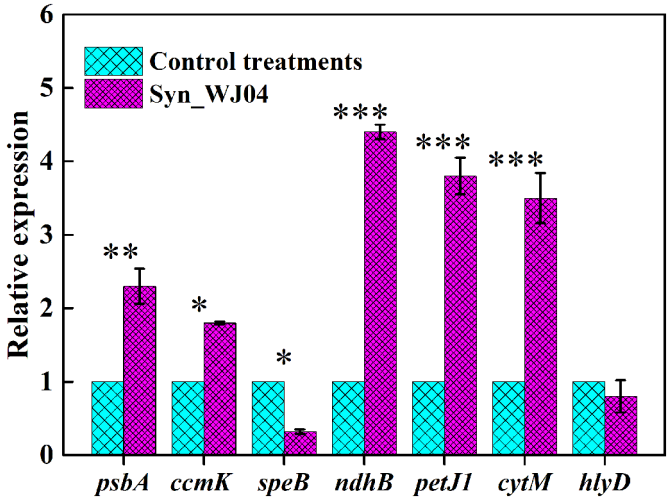

Fig. 4. Mean relative expression (± S.E., n = 6) with RT-qPCR measurements of *Synechocystis* genes in the control (axenic *Synechocystis*) and coculture treatments (Syn_WJ04). *P*-value (Student's *t*-test): "*" $P < 0.05$, "**", $P < 0.01$, "***", $P < 0.001$.

distance for more effective electron transfer among algae, bacteria and electrodes [37]. Although higher current density was detected in the coculture treatments, a systematic explanation was not provided for this phenomenon. Thus, more studies were performed to clarify the variety of bacteria present and their role in the cocultured pMFCs.

3.2. Changes in the compositions of bacterial communities in the contaminated pMFCs

The bacterial community compositions are shown in Fig. 2, and the data have been submitted to the NCBI under accession numbers SRR6279428-SRR6279433. Sequence analyses showed that the dominant bacteria community symbiotic with algae distinctly changed during the cocultivation. At the beginning of the experiment (day 0), *Aquimonas* accounted for 32.6% of all bacteria, *Pseudomonas* accounted for 22.2%, and *Methyloversatilis* accounted for 9.8%, revealing that these were the three dominant genera in the coculture treatments. After 10 days of coculturing, the heterotrophic bacteria community compositions changed. *Hydrogenophaga* had an absolute predominance (58.9%) on day 10. Notably, *Hydrogenophaga* had an abundance of approximately 60% in the coculture treatments. A previous study

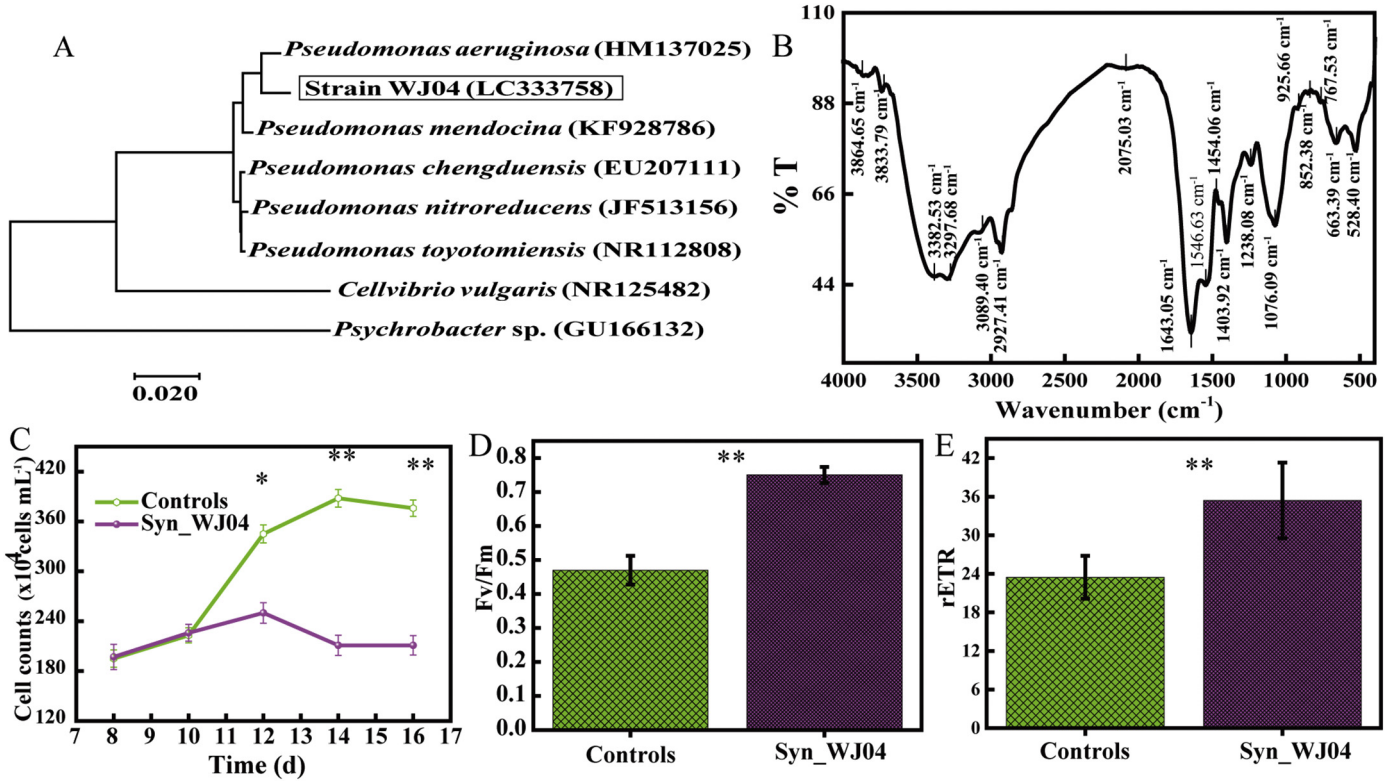

Fig. 3. Interactions between *Synechocystis* and heterotrophic bacteria. (A) Neighbor-joining phylogenetic tree and the phylogenetic position of strain WJ04; (B) FT/IR spectra of the metabolites of strain WJ04; (C) mean (± S.E., n = 6) growth rate of algae with the strain WJ04; (D) mean (± S.E., n = 6) effect of the strain WJ04 on photosynthetic efficiency (Fv/Fm) of algae; and (E) mean (± S.E., n = 6) relative electron transport rate (rETR) of algae. "Syn_WJ04" indicates the coculture treatments of *Synechocystis* and the strain WJ04. *P*-value (Student's *t*-test): "*" $P < 0.05$, "**" $P < 0.01$.

Table 2
Metabolite ratios between the *Synechocystis* which was cocultured with strain WJ04 that was put in dialysis bags and control treatments. The fold changes were calculated by the six repetitions of coculture and control treatments. *P*-value was analyzed by Student's *t*-test.

Pathways/metabolites	Fold change	Ratios	*P*-value
Carbohydrate metabolism			
L-Malic acid	34.95 ± 2.52	Increased	9.43E−14
Galactinol	12.86 ± 0.48	Increased	4.45E−06
Sucrose	8.55 ± 0.21	Increased	5.74E−11
Isomaltose	6.36 ± 0.48	Increased	4.67E−10
Amino acid metabolism			
4-Aminobutyric acid	43.37 ± 3.95	Increased	6.12E−12
S-methyl-5′-thioadenosine	10.00 ± 0.91	Increased	4.23E−09
L-Citrulline	9.28 ± 0.82	Increased	6.72E−06
L-Isoleucine	6.36 ± 0.67	Increased	4.67E−10
L-Glutamine	4.02 ± 0.84	Increased	8.52E−11
L-Pyroglutamic acid	3.81 ± 0.25	Increased	2.68E−11
L-Glutamate	3.65 ± 0.68	Increased	5.48E−12
2-Oxoadipic acid	2.30 ± 0.84	Increased	0.002
Betaine	0.83 ± 0.03	Decreased	0.001243
Lipid metabolism			
Glycerophosphocholine	14.61 ± 0.59	Increased	2.56E−12
LysoPC(16:0)	4.84 ± 0.71	Increased	2.33E−05
Palmitic acid	0.13 ± 0.53	Decreased	1.64E−09
alpha-Linolenic acid	0.21 ± 0.00	Decreased	1.6E−09
Oleic acid	0.01 ± 0.00	Decreased	8.36E−07
Arachidonic acid (peroxide free)	0.01 ± 0.00	Decreased	1.87E−08
Energy metabolism			
Nicotinamide	26.53 ± 1.59	Increased	0.00038
NAD^+	23.42 ± 2.94	Increased	8.23E−03
$NADP^+$	19.61 ± 0.62	Increased	0.86E−09
NADH	8.28 ± 0.63	Increased	1.03E−12
Adenosine monophosphate (AMP)	7.53 ± 1.43	Increased	1.03E−10
Adenine	7.25 ± 0.59	Increased	2.31E−09
NADPH	6.23 ± 1.22	Increased	1.72E−03
Adenosine	3.22 ± 1.04	Increased	8.51E−07
Biosynthesis of other secondary metabolites			
L-Homocysteic acid	37.90 ± 3.68	Increased	2.82E−18
gamma-Butyrolactone	30.15 ± 2.84	Increased	1.93E−12
beta-Carboline	12.69 ± 1.84	Increased	0.061631
3alpha-Mannobiose	8.10 ± 0.65	Increased	2.7E−11

indicated that *Hydrogenophaga* is a hydrogenotrophic electricigen and can utilize hydrogen as an electron donor [25]. *Synechocystis* is a type of algae that can produce hydrogen and may provide hydrogen as an electron donor for associated *Hydrogenophaga* under specific conditions [38]. Additionally, *Pseudomonas* (30.2%) and *Stenotrophomonas* (4.8%) were the other dominant genera in the coculture treatments on day 10, whereas the abundance of *Aquimonas* (1.0%) and *Methyloversatilis* (0.4%) was notably decreased. Because dominant anoxygenic photosynthetic bacteria were not detected in the cocultures, the regular pattern changes in the voltage curves of the cocultures were mainly due to algae. These electricity-producing bacteria, such as *Hydrogenophaga*, *Pseudomonas* and *Stenotrophomonas*, can contribute electrons to the anode and enhance the current generation of pMFCs. However, whether these symbiotic bacteria can influence the electron output of *Synechocystis* was not clarified, and pure bacteria had to be isolated to investigate the interactions between algae and bacteria in the anode.

3.3. Interactions between Synechocystis and the strain WJ04

The bacteria strain WJ04 (accession no. LC333758) was isolated and purified from cocultures, and its identity was purified and confirmed with the neighbor-joining algorithm in MEGA 5.0 (Fig. 3A) with BLAST results of the 16S rRNA gene from GenBank. Strain WJ04 is affiliated with the genus *Pseudomonas* with 99% similarity to *Pseudomonas aeruginosa* (HM137025). *Pseudomonas* sp. was a dominant bacterial community member at day 10 and has a cell-cell communication (quorum sensing) system that uses the electron shuttle phenazines [27]. These results demonstrate that the dominant bacterium in the cocultures, *Pseudomonas* sp. WJ04, was successfully isolated. *P. aeruginosa* is a model bacterium that produces electrochemically active compounds for mediated electron transfer and contributes current to cocultured pMFCs (Fig. S3). The metabolites of the stain WJ04 were analyzed by FT/IR spectroscopy, and the results showed that the metabolites of strain WJ04 had strong peaks at 3200–3400 cm^{-1} (VS) and 1500–1600 cm^{-1} (VS), indicating that abundant complex multimolecular associations, amides and bond-stretching vibrations were produced (Fig. 3B). The peaks at 3382.53 cm^{-1} and 3297.68 cm^{-1} were obvious and attributed to a stretch of the OH groups. The apparent peaks at 2800–3000 cm^{-1} were related to CH stretching vibrations. A group of benzene rings (1546.63 cm^{-1} and 1454.06 cm^{-1}) and CN stretch vibrations (1643 cm^{-1}) appeared in the double bond-stretching vibration region (1690–1500 cm^{-1}). The peaks were consistent with the findings of a previous report that *Pseudomonas* can produce the redox shuttle phenazines [39–41]. These metabolites may affect the current density of coculture treatments. A high-performance liquid chromatography system also detected the increasing phenazine concentrations in the cocultures of *Synechocystis* and *Pseudomonas* (Fig. S4). These results further verified that symbiotic bacteria in coculture treatments had the ability to influence the current density of cocultured pMFCs.

Photosynthetic algae can be used as electron donors in the anode with less energy consumption than bacteria, and many studies have been performed to obtain a high current density and high algae production using algae-bacteria cocultivation [42]. However, no systematic studies have elucidated the interaction mechanism between algae and bacteria in the anode. Strain WJ04 can influence *Synechocystis* growth, photosynthetic efficiency, relative electron transport rates and current density. The cell counts of *Synechocystis* were remarkably increased in the cocultures with strain WJ04 compared with the control cultures, and the bacteria inhibited algal growth after cocultivation for 9 days (Fig. 3C). After 8 days of cocultivation, strain WJ04 significantly stimulated the photosynthetic activities of *Synechocystis* as evidenced by the significant increase of Fv/fm and the electron transport rate at 14.0% and 50.9%, respectively (Fig. 3D & E). Strain WJ04 can stimulate the photosynthetic process and effect electron transfer rates. Current density was significantly increased in the cocultures, with a maximum increase of 8.3 fold compared to the control cultures (Fig. S5). The regulated diurnal variation reappeared in the cocultures of *Synechocystis* and strain WJ04, showing that bacteria can affect the electron output of algae in pMFCs. It is meaningful to improve the electron transfer efficiency of algae in anodes and quicken ecological processes to restore ecological environments. Our results show that the metabolites of the *Pseudomonas* sp. strain WJ04 can affect the physiology of *Synechocystis* and electron transfers in the anode.

3.4. Strain WJ04 regulates the gene expression in algae

Seven algae genes at day 10 were detected by RT-qPCR, and these genes are involved in photosynthesis and energy metabolism (Fig. 4). The expression of the gene *ccmK* encoding a CO_2-concentrating protein was 1.8-fold higher in the cocultures than the control cultures. The other genes that were upregulated in the cocultures of *Synechocystis* and strain WJ04 were as follows: *psbA* (upregulated 2.3 fold), which encodes photosystem II P680 chlorophyll apoproteins and photosystem II manganese-stabilizing polypeptides; *ndhB*, which encodes a subunit of the type I NADH dehydrogenase; *petJ1*, which encodes a putative second c-type cytochrome; and *cytM*, which is involved in NADH or mobile electron transport proteins synthesis [43,44]. Additionally, the gene *hlyD*, which is related to cellular processes, was downregulated in the coculture treatments compared with the control treatments, which is consistent with the aforementioned results (Fig. 2D), showing that when *Synechocystis* was cocultured with strain WJ04, the algal growth

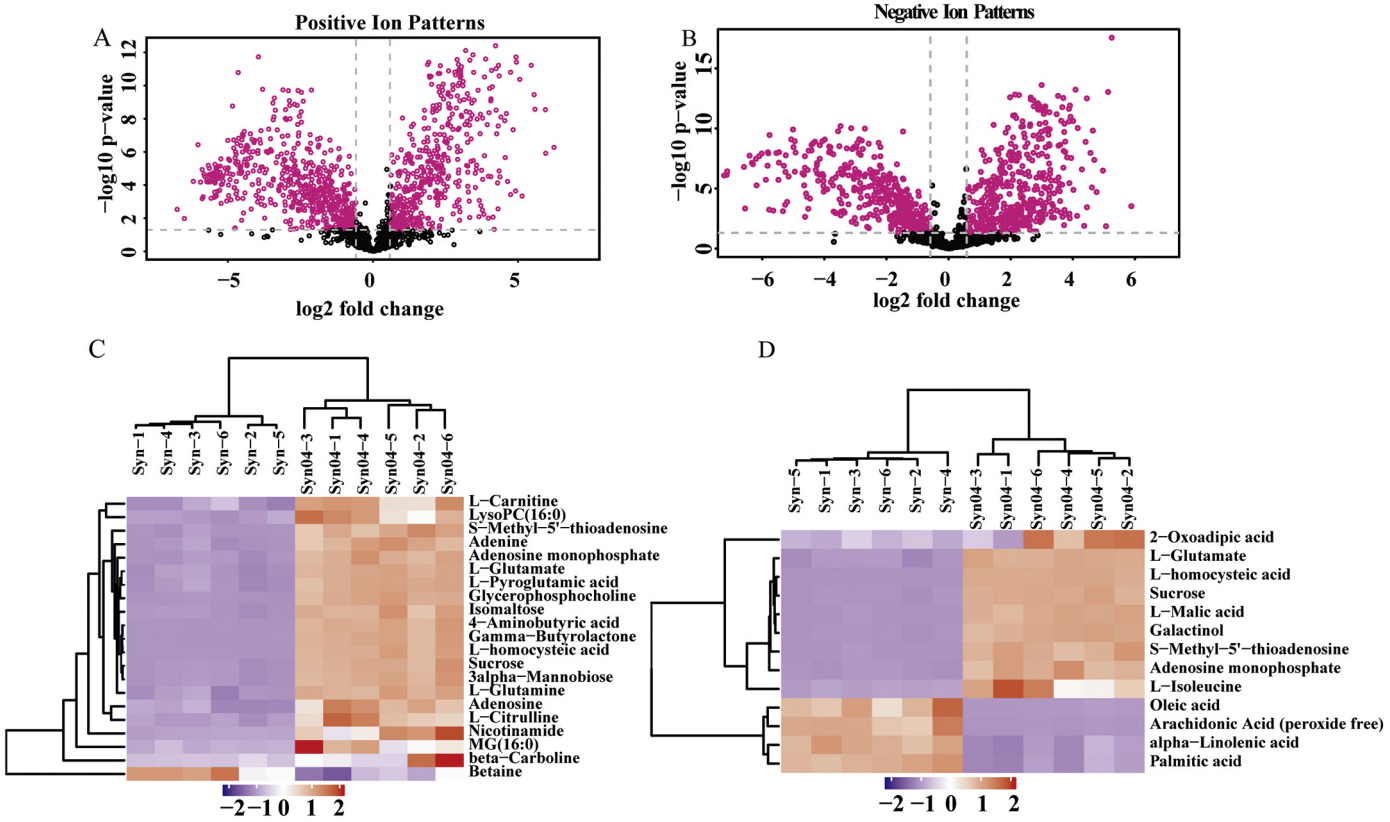

Fig. 5. Volcano plots and hierarchical clustering of differential metabolites. Volcano plot with positive (A) and negative (B) ion patterns. Red plots represent the metabolites with fold change > 2.0 and *P* value < 0.05. Hierarchical clustering with positive (C) and negative (D) ion patterns. "Syn_" represents the axenic *Synechocystis* as control treatments and their six replications; "Syn04_" represents the coculture of *Synechocystis* and the strain WJ04 and their six replications. (For interpretation of the references to color in this figure legend, the reader is referred to the web version of this article.)

rate declined after 9 days of cocultivation. The gene *speB*, which encodes a fatty acid desaturase, was also downregulated in the cocultures, and this finding is consistent with the results of the metabolomics analysis (Table 2), thus showing that levels of fatty acid-related metabolites were decreased in the cocultures. Thus, strain WJ04 can regulate the gene expression of algae and further affect the metabolic processes in algal cells. The change in metabolite production may influence the current generations of algal pMFCs.

3.5. Strain WJ04 stimulates algal metabolism production

Metabolomics analyses by ultra-performance LC-TOF-MS showed differences in a total of 183 metabolites between the control and coculture treatments, and these metabolites were related to glycometabolism, oxidative phosphorylation, the tricarboxylic acid cycle, amino acid metabolism, fatty-acid metabolism and other processes. Potential marker metabolites (*F.C.* > 2.0 and *P* value < 0.05) were screened using a univariate analysis, and volcano plots were constructed to show the remarkable differences of the metabolites in axenic algae compared to the algae cocultured with strain WJ04 (Fig. 5A & B). Thirty-two differential metabolites were found in the two treatments based on the variable importance for the projection, which was determined using a discriminant partial least squares analysis by scaling the influence and expression patterns of metabolites on the ability to classify and interpret the samples. Hierarchical clustering was used to precisely screen the differential metabolites. In the study, the treatments were replicated, and the clustering of the results showed that the identified differential metabolites were reasonable and accurate (Fig. 5C & D). The concentrations of twenty-two metabolites from *Synechocystis* cells were particularly increased in the cocultures, and the concentrations of five metabolites were decreased. The roles and related metabolic pathways of these differential metabolites in algae cells are shown in Table 2. The increased metabolites strengthened the processes of amino acid and nicotinamide metabolism but not fatty acid metabolism. Specifically, the concentrations of NAD^+, NADH, $NADP^+$ and NADPH were increased by 23.42 fold, 8.28 fold, 19.60 fold and 6.23 fold, respectively, in cocultures compared to pure culture. L-pyroglutamic acid (37.90-fold increase) was used to synthetize proton-pumping proteins in the cytomembrane that can transfer protons from NADH/NADPH to outside the cells. These extra protons in the anode can then be transferred into the cathode through the exchange membrane. The remarkable increase or decrease in differential metabolites related to carbohydrate metabolism, amino acid metabolism, lipid metabolism and energy metabolism provide more opportunities for electron production, including current generation. Because these differential metabolites may directly affect the electron transfer of algae, the metabolites with *F.C.* ≥ 10.00 were added into pMFCs to detect their effects on current production.

3.6. Metabolites regulate current generation of algae

The standards of the metabolites (with *F.C.* ≥ 10.00) were added to the algal culture to detect their effects on pMFC current production. Except for nicotinamide, L-homocysteic acid and 4-aminobutyric acid, other differential metabolites had no remarkable influence on current density. Nicotinamide, L-homocysteic acid and 4-aminobutyric acid were added into pure *Synechocystis* cultures with 0.1 mg L^{-1} concentrations. The growth rates of *Synechocystis* cells in the cocultures were below those in the control cultures. The metabolites inhibited algal growth (Fig. S6). Compared with nicotinamide and L-homocysteic acid, the inhibition of algal growth by 4-aminobutyric acid was remarkable. Compared with the inhibition of growth, the current

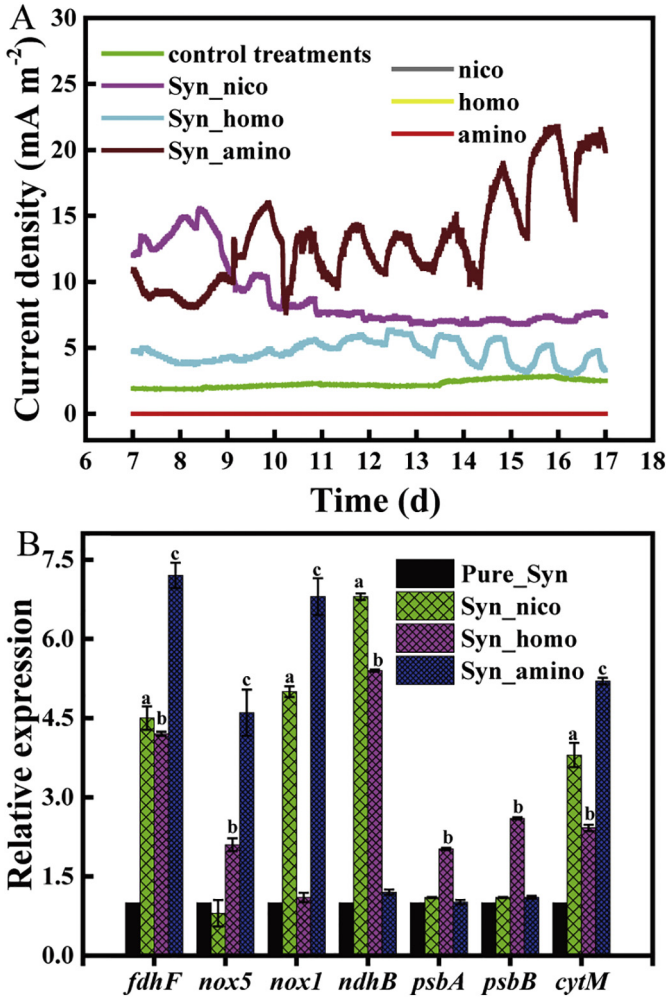

Fig. 6. Influence of metabolites on *Synechocystis* (Syn). (A) Mean (n = 6) current density of pMFCs with nicotinamide (nico), L-homocysteric acid (homo), and 4-aminobutyric acid (amino); and (B) RT-qPCR measurements of transcript abundance (n = 6). Different letters represent significant differences between pure_syn and cocultures.

densities in cocultures with metabolites were higher than those in the control treatments (Fig. 6A). Nicotinamide remarkably increased the electron output of *Synechocystis* in the cocultures and improved the current density by 7.6 fold, 4-aminobutyric acid enhanced the current density by 12.2 fold and L-homocysteic acid increased the current density by 6.1 fold compared to the control treatments. When nicotinamide, 4-aminobutyric acid and L-homocysteic acid were added into the pMFCs without algae, no current was detected. Moreover, the RT-qPCR analysis showed that the expression of the gene *fdhF* in the cocultures to which nicotinamide, L-homocysteic acid, and 4-aminobutyric acid was upregulated by 4.5 fold, 4.1 fold and 7.4 fold, respectively. *fdhF* encodes an NADP-dependent formate dehydrogenase that converts formate to CO_2 with the regeneration of NADH from $NADP^+$ (Fig. 6B). The genes *nox5* and *nox1* were upregulated by 7.3 fold and 4.5 fold respectively, in the cocultures receiving nicotinamide; by 2.2 fold and 3.4 fold, respectively, in the cocultures receiving L-homocysteic; and by 4.4 fold and 6.3 fold, respectively, in the cocultures receiving 4-aminobutyric acid, indicating that NADPH oxidases were more active in the cocultures than the control cultures. Additionally, the *ndhB* gene encoding a subunit of the type I NADH dehydrogenase and *cytM* were notably upregulated in the cocultures receiving L-homocysteic acid (2.7 fold and 2.9 fold, respectively), which lead to the increased synthesis of NADH or mobile electron transport proteins [43–45]. The upregulated *Synechocystis* genes could the accelerate electron transfer rate to provide enough electron carriers for transferring protons into the cathode. The genes *psbA* and *psbB* encoding photosystem II P680 chlorophyll apoprotein and photosystem II manganese-stabilizing polypeptide were also notably upregulated, meaning that algal photosynthesis played an important role in electron production in all cocultures. The results showed that nicotinamide, L-homocysteic acid and 4-aminobutyric acid can affect the growth of algae and upregulate the current production of algal pMFCs. Those results further verified that bacteria strain WJ04 can enhance the current generation of algal pMFC by stimulating the production of metabolites (e.g., nicotinamide, L-homocysteic acid and 4-aminobutyric acid).

4. Conclusions

A 12.6-fold higher voltage was found in bacterially contaminated pMFCs than the control treatments (axenic pMFCs). In the contaminated pMFCs, *Synechocystis* released electrons into anodic solution and *Pseudomonoas* sp. strain WJ04 also contributed extra electrons to improve the voltage output. Moreover, *Pseudomonans* sp. strain WJ04 regulated the bioprocess of algae and accelerated the synthesis of more differential metabolites, such as nicotinamide, L-homocysteic acid and 4-aminobutyric acid, to improve the algal electron release rates and further enhance the pMFC current density. The results of this study explicate the process by which current generation of contaminated pMFCs was enhanced, i.e., electricity production by bacteria and the increased production of algal metabolites, and provide reliable evidence for achieving high bioelectricity generation through the utilization of algal-bacterial interactions.

Acknowledgements

We thank Dr. Fanghua Liu (Yantai Institute of Coastal Zone Research, Chinese Academy of Sciences) for providing suggestions at the beginning of this study and Dr. Fang Dong (Yantai Institute of Coastal Zone Research, Chinese Academy of Sciences) for providing assistance on the FT/IR spectra analyses. This work was supported by the National Natural Science Foundation of China (31600370 and 41373100), Science and Technology Plan of Yantai City (2018ZHGY080 and 2018ZHGY083), and the Strategic Priority Research Program of the Chinese Academy of Sciences (XDA23050203).

Statement of informed Consent, Human/Animal Rights, if any, for the work described. No conflicts, informed consent, or human or animal rights are applicable.

Author contributions

All authors contributed in the design of the experiment. W.J. Wang performed the experiment, analyzed the data and wrote the initial manuscript. Y.Q. Sheng performed a critical revision of the manuscript. All authors approved the final submitted manuscript.

Conflict of interest

All authors approve this submission, and there are no conflicts of interest in the publication of the manuscript.

References

[1] A. Gärdes, M.H. Iversen, H.P. Grossart, U. Passow, M.S. Ullrich, Diatom-associated bacteria are required for aggregation of *Thalassiosira weissflogii*, The ISME journal 5 (2011) 436.
[2] A. Kouzuma, K. Watanabe, Exploring the potential of algae/bacteria interactions, Curr. Opin. Biotech. 33 (2015) 125–129.
[3] M. Haumann, P. Liebisch, C. Müller, M. Barra, M. Grabolle, H. Dau, Photosynthetic O_2 formation tracked by time-resolved X-ray experiments, Science 310 (2005)

1019–1021.
[4] B.G. Moore, R.G. Tischer, Extracellular polysaccharides of algae: effects on life-support systems, Science 145 (1964) 586–587.
[5] G.J. Doucette, Interactions between bacteria and harmful algae: a review, Nat. Toxins 3 (1995) 65–74.
[6] T.M. Mata, A.A. Martins, N.S. Caetano, Microalgae for biodiesel production and other applications: a review, Renew. Sust. Energ. Rev. 14 (2010) 217–232.
[7] C.Q. Arita, Ö. Yilmaz, S. Barlak, K.B. Catton, J.C. Quinn, T.H. Bradley, A geographical assessment of vegetation carbon stocks and greenhouse gas emissions on potential microalgae-based biofuel facilities in the United States, Bioresour. Technol. 221(2016) 270–275.
[8] M. Rosenbaum, Z. He, L.T. Angenent, Light energy to bioelectricity: photosynthetic microbial fuel cells, Curr. Opin. Biotech. 21 (2010) 259–264.
[9] J. Ma, Z. Wang, J. Zhang, T.D. Waite, Z. Wu, Cost-effective *Chlorella* biomass production from dilute wastewater using a novel photosynthetic microbial fuel cell (PMFC), Water Res. 108 (2017) 356–364.
[10] R.B. Song, K. Yan, Z.Q. Lin, J.S.C. Loo, L.J. Pan, Q.C. Zhang, J.R. Zhang, J.J. Zhu, Inkjet-printed porous polyaniline gel as an efficient anode for microbial fuel cells, J. Mater. Chem. A 4 (2016) 14555–14559.
[11] L.P. Wang, Q.R. Shen, G.H. Yu, W. Ran, Y.C. Xu, Fate of biopolymers during rapeseed meal and wheat bran composting as studied by two-dimensional correlation spectroscopy in combination with multiple fluorescence labeling techniques, Bioresour. Technol. 105 (2012) 88–94.
[12] J.C.F. Ortiz-Marquez, M. Do Nascimento, J.P. Zehr, L. Curatti, Genetic engineering of multispecies microbial cell factories as an alternative for bioenergy production, Trends Biotechno 31 (2013) 521–529.
[13] V. Mishra, A. Dubey, S.K. Prajapti, Algal biomass pretreatment for improved biofuel production, Algal Biofuels, Springer, Cham, 2017, pp. 259–280.
[14] R. Xiao, Y. Zheng, Overview of microalgal extracellular polymeric substances (EPS) and their applications, Biotechnology Adv 34 (2016) 1225–1244.
[15] P. Gäbelein, L. Mosebach, M. Hippler, Bioenergetic pathways in the chloroplast: photosynthetic electron transfer, Chlamydomonas: Molecular Genetics and Physiology, Springer, Cham, 2017, pp. 97–134.
[16] D. Pils, G. Schmetterer, Characterization of three bioenergetically active respiratory terminal oxidases in the cyanobacterium *Synechocystis* sp. strain PCC 6803, FEMS Microbiol. Lett. 203 (2001) 217–222.
[17] P. Zhang, M. Eisenhut, A.M. Brandt, D. Carmel, H.M. Silén, I. Vass, Y. Allahverdiyeva, T.A. Salminen, E.M. Aro, Operon flv4-flv2 provides cyanobacterial photosystem II with flexibility of electron transfer, Plant Cell 24 (2012) 1952–1971.
[18] S.A. Amin, L.R. Hmelo, H.M. Van Tol, B.P. Durham, L.T. Carlson, K.R. Heal, R.L. Morales, C.T. Berthiaume, M.S. Parker, B. Djunaedi, A.E. Ingalls, M.R. Parsek, M.A. Moran, E.V. Armbrust, Interaction and signaling between a cosmopolitan phytoplankton and associated bacteria, Nature 522 (2015) 98.
[19] D.H. Cho, R. Ramanan, J. Heo, J. Lee, B.H. Kim, H.M. Oh, H.S. Kim, Enhancing microalgal biomass productivity by engineering a microalgal–bacterial community, Bioresour. Technol. 175 (2015) 578–585.
[20] K.E. Helliwell, J. Pandhal, M.B. Cooper, J. Longworth, U.J. Kudahl, D.A. Russo, E.V. Tomsett, F. Bunbury, D.L. Salmon, N. Smirnoff, P.C. Wright, A.G. Smithe, Quantitative proteomics of a B_{12}-dependent alga grown in coculture with bacteria reveals metabolic tradeoffs required for mutualism, New Phytol. 217 (2018) 599–612.
[21] A.S. Zevin, B.E. Rittmann, R. Krajmalnik-Brown, The source of inoculum drives bacterial community structure in *Synechocystis* sp. PCC6803-based photobioreactors, Algal Res. 13 (2016) 109–115.
[22] N. Fernandes, R.J. Case, R. Longford, M.R. Seyedsayamdost, P.D. Steinberg, S. Kjelleberg, T. Thomas, Genomes and virulence factors of novel bacterial pathogens causing bleaching disease in the marine red alga *Delisea pulchra*, PLoS One 6 (2011) e27387.
[23] Y. Park, K.W. Je, K. Lee, S.E. Jung, T.J. Choi, Growth promotion of *Chlorella ellipsoidea* by co-inoculation with *Brevundimonas* sp. isolated from the microalga, Hydrobiologia 598 (2008) 219–228.
[24] W.J. Wang, H. Shen, P.L. Shi, J. Chen, L.Y. Ni, P. Xie, Experimental evidence for the role of heterotrophic bacteria in the formation of *Microcystis* colonies, J. Appl. Phycol. 28 (2016) 1111–1123.
[25] Z.I. Kimura, S. Okabe, Acetate oxidation by syntrophic association between *Geobacter sulfurreducens* and a hydrogen-utilizing exoelectrogen, The ISME Journal 7 (2013) 1472.
[26] P.T. Ha, S.R. Lindemann, L. Shi, A. Dohnalkova, J.K. Fredrickson, M.T. Madigan, H. Beyenal, Syntrophic anaerobic photosynthesis via direct interspecies electron transfer, Nat. Commun. 8 (2017) 13924.
[27] J.M. Pisciotta, Y. Zou, I.V. Baskakov, Role of the photosynthetic electron transfer chain in electrogenic activity of cyanobacteria, Appl. Microbiol. Biot. 91 (2011) 377–385.
[28] Y. Zou, J. Pisciotta, R.B. Billmyre, I.V. Baskakov, Photosynthetic microbial fuel cells with positive light response, Biotechnol. Bioeng. 104 (2009) 939–946.
[29] G.C. Gerloff, G.P. Fitzgerald, F. Skoog, The isolation, purification, and culture of blue-green algae, Am. J. Bot. 37 (1950) 216–218.
[30] H. Shen, Y. Niu, P. Xie, M. Tao, X.I. Yang, Morphological and physiological changes in Microcystis aeruginosa as a result of interactions with heterotrophic bacteria, Freshw. Biol. 56 (2011) 1065–1080.
[31] I. Krohn-Molt, M. Alawi, K.U. Förstner, A. Wiegandt, L. Burkhardt, D. Indenbirken, M. Thieß, A. Grundhoff, J. Kehr, A. Tholey, W.R. Streit, Insights into microalga and bacteria interactions of selected phycosphere biofilms using metagenomic, transcriptomic, and proteomic approaches, Front. Microbiol. 8 (2017) 1941.
[32] T.T. Zhang, L.X. Zhang, W.T. Su, P. Gao, D.P. Li, X.H. He, Y.S. Zhang, The direct electrocatalysis of phenazine-1-carboxylic acid excreted by *Pseudomonas alcaliphila* under alkaline condition in microbial fuel cells, Bioresour. Technol. 102 (2011) 7099–7102.
[33] M. Lee, J. Hong, B. Lee, K. Ku, S. Lee, C.B. Park, K. Kang, Multi-electron redox phenazine for ready-to-charge organic batteries, Green Chem. 19 (2017) 2980–2985.
[34] G. Lentini, D. Franco, E. Fazio, L.M. De Plano, S. Trusso, S. Carnazza, F. Neri, S.P.P. Guglielmino, Rapid detection of *Pseudomonas aeruginosa* by phage-capture system coupled with micro-Raman spectroscopy, Vib. Spectroscopy 86 (2016) 1–7.
[35] H. Song, M. Lavoie, X.J. Fan, H.N. Tan, G.F. Liu, P.F. Xu, Z.W. Fu, H.W. Paerl, H.F. Qian, Allelopathic interactions of linoleic acid and nitric oxide increase the competitive ability of *Microcystis aeruginosa*, The ISME Journal 11 (2017) 1865.
[36] X. Li, T. Liu, K. Wang, T.D. Waite, Light-induced extracellular electron transport by the marine Raphidophyte *Chattonella marina*, Environ. Sci. Technol. 49 (2015) 1392–1399.
[37] G. Reguera, K.D. McCarthy, T. Mehta, J.S. Nicoll, M.T. Tuominen, D.R. Lovley, Extracellular electron transfer via microbial nanowires, Nature 435 (2005) 1098.
[38] A.S. Commault, O. Laczka, N. Siboni, B. Tamburic, J.R. Crosswell, J.R. Seymour, P.J. Ralph, Electricity and biomass production in a bacteria-Chlorella based microbial fuel cell treating wastewater, J. Power Source 356 (2017) 299–309.
[39] Y.C. Yong, Y.Y. Yu, C.M. Li, J.J. Zhong, H. Song, Bioelectricity enhancement via overexpression of quorum sensing system in *Pseudomonas aeruginosa*-inoculated microbial fuel cells, Biosens. Bioelectron. 30 (2011) 87–92.
[40] K. Venkataraman, N. Boon, M. Höfte, W. Verstraete, Microbial phenazine production enhances electron transfer in biofuel cells, Environ. Sci. Technol. 39 (2005) 3401–3408.
[41] A. Venkataraman, M.A. Rosenbaum, S.D. Perkins, J.J. Werner, L.T. Angenent, Metabolite-based mutualism between *Pseudomonas aeruginosa* PA14 and *Enterobacter aerogenes* enhances current generation in bioelectrochemical systems, Energy Environ. Sci. 4 (2011) 4550–4559.
[42] E.H. Burrows, F.W. Chaplen, R.L. Ely, Optimization of media nutrient composition for increased photofermentative hydrogen production by *Synechocystis* sp. PCC 6803, Int. J. Hydrogen Energ. 33 (2008) 6092–6099.
[43] S.J. Berríos-Rivera, G.N. Bennett, K.Y. San, Metabolic engineering of Escherichia coli: increase of NADH availability by overexpressing an NAD^+-dependent formate dehydrogenase, Metab. Eng. 4(2002) 217–229.
[44] L. Zhang, B. McSpadden, H.B. Pakrasi, J. Whitmarsh, Copper-mediated regulation of cytochrome c553 and plastocyanin in the cyanobacterium *Synechocystis* 6803, J. Biol. Chem. 267 (1992) 19054–19059.
[45] C. Hervé, T. Tonon, J. Collén, E. Corre, C. Boyen, NADPH oxidases in Eukaryotes: red algae provide new hints, Curr. Genet. 49 (2006) 190–204.